

1.3 μm GaSb Metal–Semiconductor–Metal Photodetectors

Sandip Tiwari, M. C. Hargis, Y. Wang, M. C. Teich, and Wen I. Wang

Abstract—Metal–semiconductor–metal photodetectors employing GaSb active regions and $\text{Al}_{0.5}\text{Ga}_{0.5}\text{Sb}$ barrier-enhancing abrupt regions have been fabricated on InP substrates to assess the role of hole velocity and to compare with similar photodetectors made using $\text{Ga}_{0.47}\text{In}_{0.53}\text{As}$ active region. Devices exhibit photoresponse in the 0.2–0.65 A/W range, dark currents of $\approx 10^{-6}$ A at 300 K and $\approx 10^{-10}$ A at 77 K for $25 \times 25 \mu\text{m}^2$ area, and have a voltage-sensitive 3-dB bandwidth exceeding ≈ 1 GHz at 300 K and 10 GHz at 77 K. The enhanced barrier heights are estimated to be ≈ 0.30 eV. The fall time continues to be the significant component of time delay; its temperature dependence indicates that the hole velocities do improve significantly at lower temperatures. The 300 K behavior appears to be dominated by defect and impurity densities, and the effects of abrupt barriers. The larger than expected dark currents are believed to result from defects associated with lattice mismatch.

$\text{Ga}_{0.47}\text{In}_{0.53}\text{As}$ has been the III–V semiconductor of choice for 1.3 and 1.5 μm photodetectors (see, e.g., [1], [2]) for integrated applications. Metal–semiconductor–metal (MSM) photodetectors, using $\text{Ga}_{0.47}\text{In}_{0.53}\text{As}$ active region, have exhibited large bandwidths (≥ 5 GHz), when biased at large voltages (≥ 10 V) [3]. These large bias voltages are required to enhance the velocity of holes as well as their emission across the metal–semiconductor barrier region. Optimum performance requires a compromise between lowering of the barrier to achieve smaller hole pile-up together with efficient hole collection, and the resulting increase in dark current. Thus, hole transport and storage are central to the operation of MSM photodetectors. GaSb is an alternative direct gap semiconductor with a bandgap of 0.725 eV and a hole mobility of $\approx 700 \text{ cm}^2 \cdot \text{V}^{-1} \cdot \text{s}^{-1}$ at 300 K for undoped material. GaSb, like $\text{Ga}_{0.47}\text{In}_{0.53}\text{As}$, has a high-absorption coefficient for 1.3 and 1.5 μm radiation. The Fermi-level at a $\text{Ga}_{0.47}\text{In}_{0.53}\text{As}$ surface pins closer to the conduction band and at the GaSb surface pins closer to the valence band. The latter property should be expected to lead to higher dark currents, a reason perhaps for the lack of exploration of this material for detectors. However, with the use of barrier-enhancing $\text{Al}_{1-x}\text{Ga}_x\text{Sb}/\text{GaSb}$ heterostructure, it is expected that the dark current would improve while the lower effective hole mass in the alloy systems employing GaSb would continue to

result in improved hole collection properties. This improvement in hole collection, a higher hole velocity, and its close lattice matching to InAs, which offers the possibility of a n-channel as well as a complementary FET technology [4]–[7], serves as a rationale for the investigation of GaSb for photodetectors.

STRUCTURE

The material structure, grown by molecular beam epitaxy, consists of a semi-insulating InP substrate, a $\text{Al}_{0.5}\text{Ga}_{0.5}\text{Sb}$ buffer layer which is 2 μm thick, a GaSb active layer which is 1.5 μm thick, a $\text{Al}_{0.5}\text{Ga}_{0.5}\text{Sb}$ barrier layer which is 500 Å thick, and a thin overlayer of GaSb which is 50 Å thick. Although the structure is nominally undoped, it has a net background of n-type with a mobility of $5450 \text{ cm}^2 \cdot \text{V}^{-1} \cdot \text{s}^{-1}$ and a sheet carrier density of $2.6 \times 10^{12} \text{ cm}^{-2}$ which is equivalent to a carrier density of $\approx 4 \times 10^{16} \text{ cm}^{-3}$. Interdigitated-finger structures with finger lengths and finger spacings varying in the 1–4 μm range and finger widths varying in the 25–90 μm range were fabricated using silicon nitride as a dielectric layer, aluminum as a metal barrier, and titanium–platinum–gold as interconnect metal. Aluminum exhibits the smallest dark currents of various metallurgies attempted and will be reported on here.

RESULTS AND DISCUSSION

Fig. 1 shows the modulation response, at 300 K, of a large area detector at 1.3 μm wavelength. The 3-dB device response bandwidth exceeds 1.0 GHz at a bias voltage of 2.5 V. The devices exhibit dark currents of $\approx 1 \mu\text{A}$ or larger. We will summarize this later in our discussion of temperature-dependent behavior. The consequence of the large dark current, however, is a bias-dependent low frequency gain. It is small at the bias of Fig. 1, but becomes larger with increase in bias beyond ≈ 3 V. The bandwidths are similar to those observed with similar $\text{Ga}_{0.47}\text{In}_{0.53}\text{As}$ MSM structures at similar low bias voltages; the evidence here regarding the role of hole velocities is inconclusive.

However, a significant improvement in response does occur near 77 K as shown in the temporal response of Fig. 2. The full-width-half-maximum (FWHM) of the detector response is similar to the FWHM of the incident 1.3 μm laser pulse. Indeed the measurements at 77 K are limited by the system capability, the laser has a FWHM of ≈ 23 ps, the photodetector has a FWHM of ≈ 27 ps, and the measurement system has a bandwidth of 18 GHz. In Fig. 2, the increase in hole mobility leads to an improvement in the detector response in the initial part of the carrier collection

Manuscript received November 12, 1991.

S. Tiwari and M. C. Hargis are with IBM Research Division, IBM Thomas J. Watson Research Center, Yorktown Heights, NY 10598.

Y. Wang, M. C. Teich, and W. I. Wang are with the Department of Electrical Engineering, Columbia University, New York City, NY 10011.

IEEE Log Number 9106537.

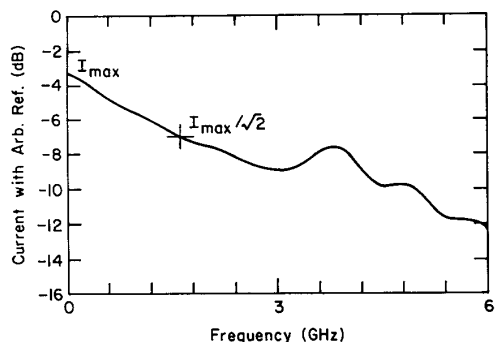


Fig. 1. The modulation response at $1.3 \mu\text{m}$ wavelength and 2.5 V bias voltage for a $90 \times 90 \mu\text{m}^2$ area MSM diode employing $2 \mu\text{m}$ finger lengths and spacings. The 3-dB device response bandwidth exceeds 1.0 GHz at a bias voltage of 2.5 V .

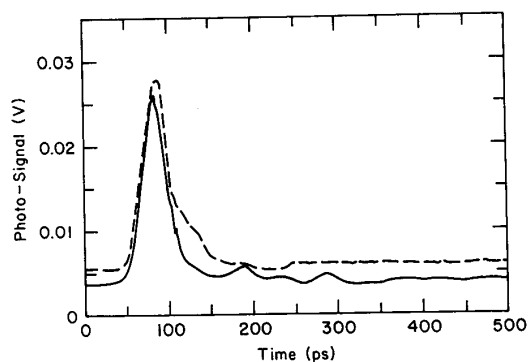


Fig. 2. The temporal response at $\approx 77 \text{ K}$ to a laser pulse with FWHM of 23 ps . The solid line shows the detected laser signal and the dashed line shows the detector signal. The GaSb MSM photodetector is biased at 5 V . The fall time of the response is 52.2 ps and the FWHM of the response is nearly the same as that of the laser pulse. The bandwidth is estimated to exceed 10 GHz .

process; the tail of the response corresponds to a velocity of $\approx 3 \times 10^6 \text{ cm}\cdot\text{s}^{-1}$ at an electric field of $\approx 2.5 \times 10^3 \text{ V}\cdot\text{cm}^{-1}$. The bandwidth of the detector, based on these measurements, exceeds 10 GHz at the bias voltage of 5 V . This is a substantial improvement over $\text{Ga}_{0.47}\text{In}_{0.53}\text{As}$ MSM detectors which typically exhibit bandwidths of factors of 3 smaller under similar bias conditions.

This low-temperature response does suggest an improvement in the characteristics of the detectors that could be attributed to the improvement in transport and storage of holes in these structures. The decrease in FWHM, largely associated with the peak response region and hence with high carrier densities in the detector, suggests both an improvement in low-field velocity of carriers which occurs due to improvements in mobility, and an insignificant effect of collection inefficiencies at these large hole carrier densities. At 300 K , the mobilities in these structures are still low, similar to those of other III-V semiconductors, perhaps due to the effects of residual defects arising from the lattice-mismatched growth and residual impurities.

The very efficient collection of holes, however, suggests

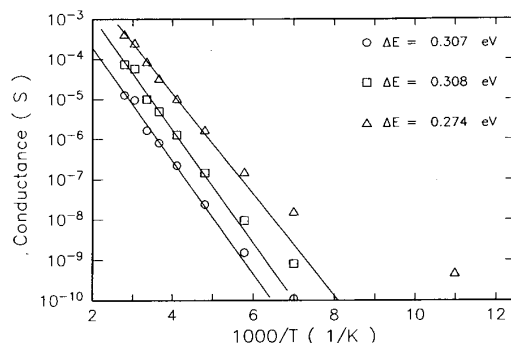


Fig. 3. Activation energy plots of zero-bias conductance for a $25 \times 25 \mu\text{m}^2$ area detector (circles), a $55 \times 50 \mu\text{m}^2$ area detector (squares), and a $90 \times 90 \mu\text{m}^2$ area detector (triangles) with equal finger lengths and spacings. Activation energies are derived from data between 358 and 243 K . At lower temperatures, tunneling effects dominate.

that the effective barrier height of these structures is probably small. Since these are back-to-back rectifying junctions, we have employed activation energy of the conductance at zero bias to obtain an effective barrier height. So long as the injection process is exponentially activated (i.e., $\propto \exp(\Delta E/kT)$ where ΔE is the effective barrier height, k is Boltzman's constant, and T is the temperature), a premise that can be tested *a posteriori*, this results in a useful parameter. Fig. 3 shows the activation energy plots of the conductance at zero bias for three different area devices. The activation energies of these structures are in the 0.27 – 0.30 eV range. Since these are n-type structures and electrons continue to be the lower mass carriers, this activation energy should correspond to electron transport. The interfacial $\text{Ga}_{0.5}\text{Al}_{0.5}\text{Sb}$ region is 500 \AA thick, is near the direct-indirect cross-over, and has an indirect bandgap of $\approx 1.3 \text{ eV}$ with X -minimum as the lowest valley. The conduction and valence band discontinuities in the $\text{Ga}_{0.5}\text{Al}_{0.5}\text{Sb}/\text{GaSb}$ system are quite symmetric, approximately 0.20 – 0.25 eV for both barriers. The barrier height of metal- $\text{Al}_{0.5}\text{Ga}_{0.5}\text{Sb}$ structure is expected to be $\approx 0.7 \text{ eV}$. The discrepancy with the measured effective barrier suggests that either a significant fraction of $\text{Al}_{0.5}\text{Ga}_{0.5}\text{Sb}$ is consumed during the fabrication process resulting in small barrier enhancement or that an alternate low-activation conduction process, such as through defects, occurs in these structures. Since the fabrication of the structure maintains a silicon-nitride layer on the structure through all stages of photolithography, the second is the most likely explanation for the low-activation energies. It perhaps occurs due to the lattice-mismatched growth on InP substrates.

Fig. 4 shows the responsivity of the detectors, at 300 K , as a function of optical intensity for various bias voltages. At low-bias voltages, the responsivity is of order of 0.2 A/W ; at high bias voltages, but low intensities, it can exceed 0.6 A/W which is close to the theoretical maximum. The intensity dependence of the responsivity is large at high bias voltages and is attributable to both the low-frequency gain and the limitations on transport placed by an abrupt barrier. Use of graded junctions should decrease the latter effect.

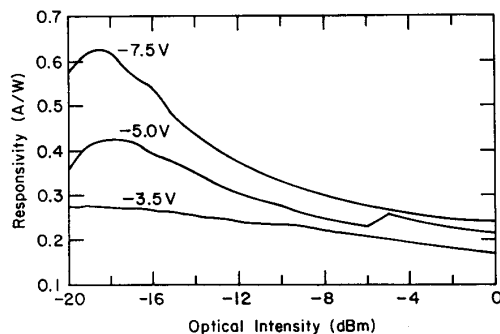


Fig. 4. Responsivity at 300 K as a function of optical intensity of 1.3 μm wavelength for various bias voltages. The responsivity varies between 0.18 and 0.63 A/W and is a function of optical intensity and applied bias.

CONCLUSIONS

We have made an initial demonstration of GaSb MSM photodetectors. These devices may be suitable for long wavelength detection. We have also presented evidence, based on low-temperature measurements, that the devices exhibit the expected properties arising from improvement in hole transport. Bandwidths exceeding 1 GHz at 300 K and 10 GHz at 77 K occur at small bias voltages. The 77 K results are

substantial improvements over similar MSM photodetectors in alternate materials. The responsivity of these structures is large, being ≈ 0.65 A/W at the peak. However, the devices still suffer from relatively large dark currents and a responsivity that is intensity-dependent.

REFERENCES

- [1] J. B. D. Soole and H. Schumacher, "InGaAs metal-semiconductor-metal photodetectors for long wavelength optical communications," *IEEE J. Quantum Electron.*, vol. QE-27, p. 737, 1991.
- [2] J. H. Burroughes and M. Hargis, "1.3 micron InGaAs MSM photodetector with abrupt InGaAs/AlGaAs interface," *IEEE Photon. Technol. Lett.*, vol. 3, p. 532, 1991.
- [3] J. H. Burroughes, D. L. Rogers, G. Arjavalingam, G. D. Pettit, and M. S. Goorsky, "Doping-induced bandwidth enhancement in metal-semiconductor-metal photodiodes," *IEEE Photon. Technol. Lett.*, vol. 3, p. 657, 1991.
- [4] L. F. Luo, R. Beresford, W. I. Wang, and H. Munekata, "Heterojunction field-effect transistors based on AlGaSb/InAs," *Appl. Phys. Lett.*, vol. 55, p. 789, 1989.
- [5] L. F. Luo, K. F. Longenbach, and W. I. Wang, "p-channel modulation-doped field-effect transistors based on AlSbAs/GaSb," *IEEE Electron Device Lett.*, vol. EDL-11, p. 567, 1990.
- [6] K. Yoh, T. Moriuchi, and M. Inoue, "An InAs channel heterojunction field-effect transistor with high transconductance," *IEEE Electron Device Lett.*, vol. EDL-11, p. 526, 1990.
- [7] K. Yoh, M. Yano, H. Taniguchi, and M. Inoue, "A p-channel GaSb heterojunction field-effect transistor based on vertically integrated complementary circuit structure," presented at *18th Int. Symp. on GaAs and Related Compounds*, 1991.

Fabrication and Test of an Efficient Photovoltaic Cell for Laser Optical Power Transmission

F. X. D'Amato, J. M. Berak, and A. J. Shuskus

Abstract—An AlGaAs photocell designed for efficient optical-to-electrical power conversion of monochromatic radiation has been fabricated and tested. A power conversion efficiency of 59% and a fill factor of 82% were measured when the device was illuminated by a laser diode source at 826 nm wavelength. The conversion efficiency of the cell remained constant for optical powers up to 1.7 W (54 W/cm^2), which was the limit imposed by the intensity of the available laser diode source. Such a device is needed for use in applications that require optical power transmission to remote sensors or electrical systems.

Manuscript received September 30, 1991.
The authors are with United Technologies Research Center, East Hartford, CT 06108.
IEEE Log Number 9106241.

THERE are a number of application areas for which it is potentially advantageous to transmit electrical power from a source to a remote electrical system using optical fibers. The advantages of optical versus electrical power transmission include immunity from EMI, elimination of power leakage due to radiative losses, the ability to electrically isolate the power source from the remote system or sensor, as well as potential reduction in overall system weight due to replacement of copper wire with optical fiber. The availability of relatively low-cost, high-power laser diodes having electrical-to-optical power conversion efficiencies exceeding 50% have made such systems increasingly practical in recent years, and several groups have demonstrated the feasibility of optical power transmission using